



OPTIMIZATION OF PROCESS PARAMETERS OF WIRE ARC ADDITIVELY MANUFACTURED SS304L PARTS USING TOPSIS

¹K.V.Prasanna Kumar, ²M.P.Bharadwaj, ³A.Vasu Anil, ⁴K.Siva Kumar, ⁵K. Sreenivasa Reddy

¹UG Student, ²UG Student, ³UG Student, ⁴UG Student, ⁵Assistant Professor

Department of Mechanical Engineering,

Godavari Institute Of Engineering And Technology (A), 533296, Rajahmundry, AP, INIDA

Abstract: Ability to produce large metallic parts with low to medium complexity made wire arc additive manufacturing (WAAM) a viable alternative to the conventional manufacturing processes. Prediction and optimization of process parameters is of the paramount importance due to influence of those on the build quality and mechanical properties. In this article, WAAM manufacturing process of SS304L was investigated for the prediction and optimization of 304L stainless steel. In order to investigate the influence of voltage, current and travel speed, a L16 Taguchi experimental design was used with the geometrical characteristics of the deposit and the hardness as the response variables. The TOPSIS (Techniques for Order – Preferences by Similarity to – Ideal Solution) technique was used to determine the ideal process parameters. The data obtained indicate that travel speed has the greatest impact on WWB and HWB, while heat input has an impact on microhardness. The optimal process parameters, $V= 21.5$ V, $I= 80$ A, $TS= 200$ m/min, were obtained.

Keywords - WAAM, GMAW, SS304L, microhardness, TOPSIS.

I. INTRODUCTION

Additive manufacturing becoming more and more in demand across a range of sector and research areas [1]. Because of how quickly wire arc additive manufacturing, material deposition and building rates, WAAM is appropriate for substantial parts [2]. WAAM technology's difficulties as well as the kinds of created components are investigated to manufacture substantial metal components with high deposition rates economically [3]. The expansion of WAAM, sometimes called as energy deposition controlled by gas metal arc is being driven by the need for increased engineering structure production efficiency [4-5]. In WAAM, gas metal arc welding is included. (GMAW) method using cold metal transformation and little heat input [6].

Stainless steel is an alloy that has a high alloy content, making it appropriate for high temperatures and corrosion resistance. A frequent application for stainless steels is in the production of aerospace industries and additional subsystems [7]. An example of an austenitic stainless steel is SS304L alloy steel [8]. The composition of stainless steel is 0.027%C, 0.39%Si, 1..61%Mn, 0.025%P, 0.011%S, 8.01%Ni, 69.24%Fe, and 18.27%Cr. SS304L's low carbon content of 0.03 weight of carbide to in a tiny amount of precipitation of carbide to develop [9]. One of the author J.S.Zuback [10] states that, in the as – fabricated state, the range of hardness values among ferrous, aluminium, and nickel alloys is quite small. Few research have up to this point concentrated on forecasting and maximizing processing parameters in SS304L WAAM in order to acquire the right geometrical properties of the weld beads. Two other crucial factors for the creation of deposition routes for the WAAM process of thin – walled and thick – walled components are the width and

height of the weld beads, indicated by WWB and HWB. The effect of travel speed and wire – feed speed on WWB and HWB were examined by Youheng et al. [11]. Three process parameters were taken into account when designing the experiments: voltage (V), current (I), travel speed (TS). The answers are composed of the weld beads' width (WWB), height (HWB). The TOPSIS (Techniques for order preferences by similarity – to – ideal solution) approaches were used to determine the ideal processing parameters[12], [13], [14].

II. EXPERIMENTAL PROCEDURE

2.1. Materials

16 Samples of SS304L were created using the GMAW based WAAM at different heat inputs (J/mm) using a 3 – axis CNC manipulator fitted with welding machine. The material in coil form with a 0.8 mm wire diameter (SS304L) was used. An argon with a 99.99% purity and a 15 L/min flow rate was employed to shield the molten metal from oxidation. For each sample that was manufactured using particular process settings, four specimens were prepared for microhardness test. The 6mm width specimens were polished to a flat surface using 320, 400 and 600 grade abrasive papers in a polishing station prior to testing. This produced a smooth surface with a surface roughness (Ra) of less than 0.1 μm .

2.2. Methodology

The main goals of this work is to identify the ideal processing parameters for the WAAM of 304L stainless steel and to evaluate the impact of input parameters { V, I, TS } on the geometrical properties and microhardness of 16 single weld bead specimens.

Step 1: Determining the vickers microhardness values of test specimens. Vickers microhardness was assessed on the specimen's surface utilizing a pyramidal diamond indenter. Vickers microhardness measurements were made at randomly chosen locations on the specimen's surface within the guage length. With a dwell time of 60 sec, the microhardness at 50kg was applied. One indents were produced at the cross – sectional surface along the WAAM sample's building direction, and microhardness was measured. The vickers hardness number was calculated in terms of (kg/mm^3) by using Eq. (2.2.1):

$$\text{Vickers hardness number (VHN)} = \frac{1.854 \times P}{d^2} \quad \text{Eq.(2.2.1)}$$

Where P = load applied on the specimen = 50kg

D_1 = Diagonal length 1 (mm)

D_2 = Diagonal length 2 (mm)

d = Average diagonal length (mm)

$$d = \frac{D_1 + D_2}{2}$$

Step 2: Finding the input variables: We did multiple trials using single weld beads, taking process parameter values within suggested limits. Following few trial runs, the following value ranges for travel speed, voltage, and welding current were established: This enables the production of continuous weld beads with fewer spatters at $I = 80 - 105\text{A}$, $V = 15 - 23\text{V}$, and $\text{TS} = 200 - 350 \text{ mm/min}$.

Step 3: Planning the experiment and collection of data: Three input variables with four levels were chosen for this investigation, as shown in Table 1. 16 experimental runs of single weld beads were therefore conducted in order to collect data on the responses that were taken into consideration (i.e., WWB, HWB) and also VHN. The substrates were cooled to room temperature for the subsequent runs following each run. Table 3 displayed the experimental design and measurement outcomes.

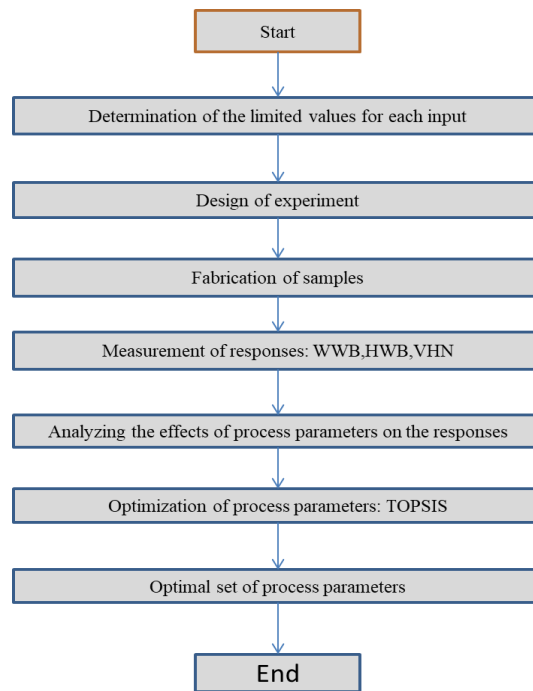


Figure 1. Methodology

Table 1. Process parameters and their levels used in the experiment

Process parameters	Levels			
	1	2	3	4
Current (A)	80	86	94	105
Voltage (V)	15	20	21.5	23
TS (mm/min)	200	250	300	350

Table 2. Experimental strategy and the response measurement outcomes

Run	Voltage (V)	Current (I)	Travel speed (mm/min)	WWB (mm)	HWB (mm)	VHN (kg/mm ²)
1	15	80	200	6.20	2.25	201.066
2	15	86	250	7.05	3.02	229.35
3	15	94	300	7.05	2.35	232.25
4	15	105	350	7.04	2.04	235.80
5	20	80	200	6.25	2.10	206.78
6	20	86	250	7.50	2.25	212.64
7	20	94	300	6.80	2.50	220.39
8	20	105	350	6.10	2.35	224.58
9	21.5	80	200	6.35	1.60	202.25
10	21.5	86	250	5.80	1.05	208.68
11	21.5	94	300	7.85	2.25	179.69
12	21.5	105	350	7.15	2.04	190.55
13	23	80	200	6.20	1.75	188.91
14	23	86	250	6.25	2.35	204.21

15	23	94	300	6.75	1.55	173.59
16	23	105	350	7.25	2.25	195.24

Step 4: Optimization of process parameters by using TOPSIS method: Technique for order preferences by similarity – to – ideal solution (TOPSIS) method, the responses were first arranged in a decision matrix $M = [y_{ij}^{(0)}]_{m \times n}$, where $y_{ij}^{(0)}$ is the initial value of the j^{th} responses in the i^{th} experiment, $1 \leq i \leq m$ and $1 \leq j \leq n$.

Second, the matrix M was normalized according to Eq.(2.2.2):

$$r_{ij} = \frac{y_{ij}^{(0)}}{\sqrt{\sum_{i=1}^m (y_{ij}^{(0)})^2}} \text{ with } i=1,2,\dots,m \text{ and } j = 1,2,\dots,n$$

Eq. (2.2.2)

Third, a set of weights $\{w_j = 1,2,\dots, n\}$ is used to compute the weighted – normalized – decision matrix, Eq.(3), where $w_j \in (0,1)$ and $\sum_{j=1}^n w_j = 1$.

$$v_{ij} = w_j r_{ij}, (i = 1,2 \dots m; j = 1,2 \dots, n)$$

Eq.(2.2.3)

The next step is to determine ideal solutions (IS) and negative – ideal solutions (NIS) based on v_{ij} , as shows in Eqs. (2.2.4) and Eq.(2.2.5), respectively.

$$IS = \{(\overset{max}{i} v_{ij} | j \in J), (\underset{i}{min} v_{ij} | j \in J) \} i = 1,2 \dots m = \{IS_1, IS_2, \dots, IS_n\}$$

Eq.(2.2.4)

$$NIS = \{(\underset{i}{min} v_{ij} | j \in J), (\overset{max}{i} v_{ij} | j \in J) \} i = 1,2 \dots, m = \{NIS_1, NIS_2, \dots, NIS_n\}$$

Eq.(2.2.5)

The distance of feasible solutions from IS or NISs is computed as Eq. (2.2.6) and Eq. (2.2.7), respectively:

$$DIS_i = \sqrt{\sum_{j=1}^n (v_{ij} - IS_j)^2}, i = 1,2, \dots, m$$

Eq.(2.2.6)

$$DNIS_i = \sqrt{\sum_{j=1}^n (v_{ij} - NIS_j)^2}, i = 1,2, \dots, m$$

Eq.(2.2.7)

Finally, the closeness degree of ideal solution $CDIS_i$ is determined by Eq. (2.2.8):

$$CDIS_i = \frac{DNIS_i}{(DIS_i + DNIS_i)}, i = 1,2 \dots m$$

Eq.(2.2.8)

The $CDIS_i$ value falls between 0 and 1. The maximum value of $CDIS_i$ corresponds to the ideal solution. The weight value of every response utilized in TOPSIS was determined by the application of the CRITIC approach. Moreover python programming is used visual studio code to carry out TOPSIS procedures.

III. RESULTS AND DISCUSSION

3.1. VHN Values obtained from microhardness test.

Table (3) shows the VHN (Vickers Hardness Number) obtained from microhardness test. The highest VHN is 235.80 kg/mm² corresponds to RUN 4 an lowest VHN is 173.59 kg/mm² corresponds to RUN 15. From Fig (2), it can be observed that the lower heat input creates the higher hardness (235.80 kg/mm²) and higher heat input creates the lower hardness (173.59 kg/mm²).

Table 3.VHN Values

Run	1	2	3	4	5	6	7	8	9	10	11	12	13	14	15	16
VHN (kg/mm ²)	201	229	232	235	206	212	220	224	202	208	179	190	188	204	173	195

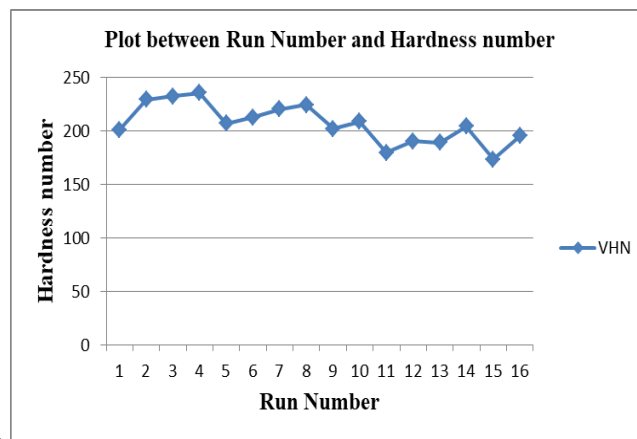


Figure 2. Plot between Run Number and VHN



Figure 3. Indentation on surface of the specimen

3.2. Optimization with TOPSIS method.

Table 4 shows results obtained using the TOPSIS method. Eqs. (2.2.2) and (2.2.3) were used to get the elements of the normalized decision matrix and the weighted normalized decision matrix, respectively. For every response, the ideal solutions (IS) are IS (WWB) = 0.11633, IS (HWB) = 0.10528, IS (VHN) = 0.02092. For every response, the negative idea solutions (NIS) are NIS (WWB) = 0.08595, NIS (HWB) = 0.03660, NIS (VHN) = 0.02092. Equations (2.2.6) and (2.2.7) are used to calculate the distance between feasible solutions and ISs or NISs (DIS_i and $DNIS_i$), respectively. As indicated by the rank in the last column of Table 4, it is determined based on the values of CDIS that the run 10 is found to be the best solution.

Table 4. Results of the computation of normalized and weighted normalized decision matrices, distance values (DIS_i and $DNIS_i$) and $CDIS_i$ values.

Run	Normalized Decision Matrix			Weighted Normalized Decision Matrix			Distances and Rank			
	WWB (mm)	HWB (mm)	VHN (kg/mm ²)	WWB (mm)	HWB (mm)	VHN (kg/mm ²)	DIS_i	$DNIS_i$	$CDIS_i$	Rank
1	0.229	0.261	0.242	0.091	0.078	0.024	0.036	0.042	0.463	8
2	0.261	0.350	0.276	0.104	0.105	0.027	0.011	0.071	0.142	16
3	0.261	0.273	0.279	0.104	0.081	0.027	0.026	0.049	0.346	14
4	0.260	0.237	0.284	0.104	0.071	0.028	0.036	0.039	0.476	6
5	0.231	0.244	0.249	0.092	0.073	0.024	0.040	0.037	0.516	5
6	0.277	0.261	0.256	0.111	0.078	0.025	0.027	0.049	0.359	12
7	0.25	0.29	0.256	0.10	0.08	0.026	0.02	0.052	0.311	15

	1	0		0	7		3			
8	0.22 6	0.27 3	0.270	0.09 0	0.08 1	0.027	0.03 4	0.045	0.431	9
9	0.23 5	0.18 5	0.243	0.09 4	0.05 5	0.024	0.05 4	0.021	0.720	2
10	0.21 4	0.12 2	0.251	0.08 5	0.03 6	0.025	0.07 5	0.004	0.946	1
11	0.29 0	0.26 1	0.216	0.11 6	0.07 8	0.021	0.02 7	0.051	0.348	13
12	0.26 4	0.23 7	0.229	0.10 5	0.07 1	0.022	0.03 6	0.039	0.474	7
13	0.22 9	0.20 3	0.227	0.09 1	0.06 1	0.022	0.05 0	0.025	0.668	4
14	0.23 1	0.27 3	0.246	0.09 2	0.08 1	0.024	0.03 3	0.045	0.421	10
15	0.25 0	0.18 0	0.209	0.10 0	0.05 4	0.020	0.05 4	0.022	0.707	3
16	0.26 8	0.26 1	0.235	0.10 7	0.07 8	0.023	0.02 8	0.047	0.378	11

Table 5. CDIS averages based on the levels of the input variables

Level	Current (A)	Voltage (V)	Table speed (mm/min)
1	0.591	0.356	0.591
2	0.467	0.404	0.467
3	0.428	0.622	0.428
4	0.439	0.438	0.439
Delta = Max - Min	0.163	0.266	0.163
Rank	2	1	2

The CDIS mean values are displayed in Table 4. They also disclose the ideal circumstance for the maximum CDIS values, which is indicated in Table 4. Current (I) = 80 A, Voltage (V) = 21.5 Volts, travel speed = 200 mm/min.

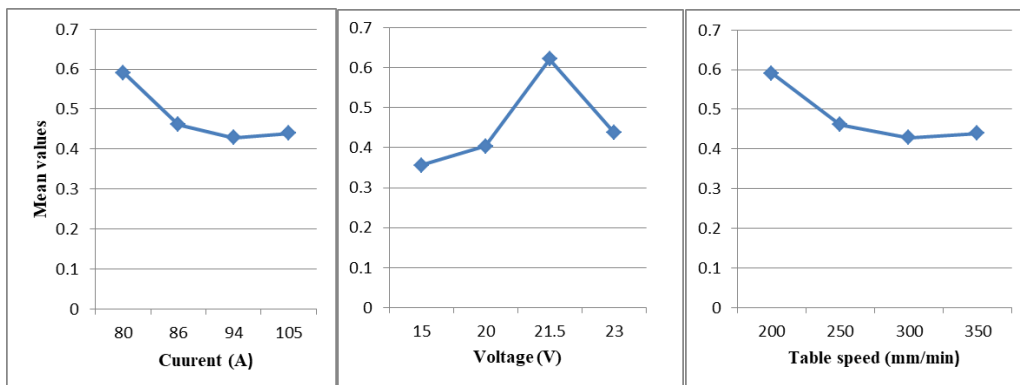


Figure 4. Effect on process parameters on CDIS

It can be seen from the data that the TOPSIS approach provide a comparable set of ideal process parameters. Therefore, based on the established optimal criteria, we may conclude that current (I) = 80 A, Voltage (V) =

21.5 V, travel speed = 200 mm/min are the ideal process parameters for the WAAM process of SS304L. These values have been utilized to construct a wall with 15 layers of single bead in order to validate the ideal process parameters. The obtained structure has a uniform width and height for every pass.



Figure 5. Single wall structure built with optimum set of parameters

IV. CONCLUSION

This study sought to determine the microhardness of the test specimens and examine the effects of process variables on the weld bead properties (such as width and height, or WWB and HWB) in the GMAW – WAAM process of 304L stainless steel. The TOPSIS approach was employed as to certain the ideal process parameters. The primary findings of this study can be summarized as follows:

- The metal undergoes thermal cycles during the WAAM process, which is why there is a drop in microhardness along the building direction. The lower heat input creates higher hardness (235 VHN). Compared to lower heat input, higher heat input creates low hardness (174 VHN), which leads to more plastic deformation
- When it comes to solving multi – objective decision – making situations, TOPSIS are an efficient option. The TOPSIS technique yields the ideal SS304L WAAM process parameters, Which are current (I) = 80 A, voltage = 21.5 V and travel speed = 200 mm/min. These values were effectively applied to the construction of a wall with 15 deposited layers. The constructed part's stable and regular geometry proves that the ideal process parameters were used.

REFERENCES

- [1] W. E. Frazier, "Metal Additive Manufacturing: A Review," J. of Materi Eng and Perform, vol. 23, no. 6, pp. 1917–1928, Jun. 2014, doi: 10.1007/s11665-014-0958-z.
- [2] Iván Taberero, A. Paskual, P. Álvarez, and A. Suárez, "Study on Arc Welding Processes for High Deposition Rate Additive Manufacturing," Procedia CIRP, vol. 68, pp. 358–362, 2018, doi: 10.1016/j.procir.2017.12.095.
- [3] D. Jafari, T. H. J. Vaneker, and I. Gibson, "Wire and arc additive manufacturing: Opportunities and challenges to control the quality and accuracy of manufactured parts," Materials & Design, vol. 202, p. 109471, Apr. 2021, doi: 10.1016/j.matdes.2021.109471.
- [4] Busachi, J. Erkoyuncu, P. Colegrove, F. Martina, and J. Ding, "Designing a WAAM Based Manufacturing System for Defence Applications," Procedia CIRP, vol. 37, pp. 48–53, 2015, doi: 10.1016/j.procir.2015.08.085.
- [5] Blakey-Milner, "Metal additive manufacturing in aerospace: A review," Materials & Design, vol. 209, p. 110008, Nov. 2021, doi: 10.1016/j.matdes.2021.110008.
- [6] Y. Li, X. Huang, I. Horváth, and G. Zhang, "GMAW-based additive manufacturing of inclined multi-layer multi-bead parts with flat-position deposition," Journal of Materials Processing Technology, vol. 262, pp. 359–371, Dec. 2018, doi: 10.1016/j.jmatprotec.2018.07.010.
- [7] Mahale, R S, Rajendrachari, S, Vasanth, S, Krishna, H, Nithin, SK, Chikkegowda, SP, Patil, A, "Technology and Challenges in Additive Manufacturing of Duplex Stainless Steels," Biointerface Res Appl Chem, vol. 12, no. 1, pp. 1110–1119, Apr. 2021, doi: 10.33263/BRIAC121.11101119.
- [8] M. A. Linger and T. M. Bogale, "Parameters optimization of tungsten inert gas welding process on 304L stainless steel using grey based Taguchi method," Eng. Res. Express, vol. 5, no. 1, p. 015013, Mar. 2023, doi: 10.1088/2631-8695/acb526.
- [9] V. Setyowati, Suheni, F. Abdul, and S. Ariyadi, "Effect of welding methods for different carbon content of ss304 and ss304l materials on the mechanical properties and microstructure," IOP Conf.

Ser.: Mater. Sci. Eng., vol. 1010, no. 1, p. 012018, Jan. 2021, doi: 10.1088/1757-899X/1010/1/012018.

- [10] J. S. Zuback and T. DebRoy, "The Hardness of Additively Manufactured Alloys," *Materials*, vol. 11, no. 11, p. 2070, Oct. 2018, doi: 10.3390/ma11112070.
- [11] F. Youheng, W. Guilan, Z. Haiou, and L. Liye, "Optimization of surface appearance for wire and arc additive manufacturing of Bainite steel," *Int J Adv Manuf Technol*, vol. 91, no. 1–4, pp. 301–313, Jul. 2017, doi: 10.1007/s00170-016-9621-1.
- [12] Y. Koli, S. Arora, S. Ahmad, Priya, N. Yuvaraj, and Z. A. Khan, "Investigations and Multi-response Optimization of Wire Arc Additive Manufacturing Cold Metal Transfer Process Parameters for Fabrication of SS308L Samples," *J. of Materi Eng and Perform*, vol. 32, no. 5, pp. 2463–2475, Mar. 2023, doi: 10.1007/s11665-022-07282-6.
- [13] S. Nipanikar, V. Sargade, and R. Guttedar, "Optimization of process parameters through GRA, TOPSIS and RSA models," *10.5267/j.ijiec*, pp. 137–154, 2018, doi: 10.5267/j.ijiec.2017.3.007.
- [14] V. T. Le et al., "Prediction and optimization of processing parameters in wire and arc-based additively manufacturing of 316L stainless steel," *J Braz. Soc. Mech. Sci. Eng.*, vol. 44, no. 9, p. 394, Sep. 2022, doi: 10.1007/s40430-022-03698-2.

